Title
Effective Two-Body Interactions

Journal
The Journal of Physical Chemistry A, 125(35)

ISSN
1089-5639

Authors
Mackie, Cameron
Zech, Alexander
Head-Gordon, Martin

Publication Date
2021-09-09

DOI
10.1021/acs.jpca.1c05677

Peer reviewed

Effective Two-Body Interactions

Cameron Mackie,[†,‡] Alexander Zech,[†] and Martin Head-Gordon[*,†,‡]

†*Department of Chemistry, University of California, Berkeley, California 94720, USA*

‡*Chemical Sciences Division, Lawrence Berkeley National Laboratory, Berkeley, California 94720, USA*

E-mail: mhg@cchem.berkeley.edu

Abstract

Cooperative or non-additive effects contribute to the pairwise non-covalent interaction of two molecules in a cluster or the condensed phase in ways that depend on the specific arrangements and interactions of the other surrounding molecules that constitute their environment. General expressions for an effective two-body interaction are presented, which are correct to increasing orders in the many-body expansion. The simplest result, correct through third order, requires only seven individual calculations, in contrast to a linear number of three-body contributions. Two applications are presented. First, an error analysis is performed on a model $(H_2O)_8$ cluster which completes the first solvation shell of a central water-water hydrogen bond. Energy decomposition analysis is performed to show that the largest effects of cooperativity on the central hydrogen bond arise from electrical polarization. Second, the nature of cooperative effects on proton transfer in an HCl + $(H_2O)_4$ cluster is characterized.

1 Introduction

Molecular gases, clusters and liquids have structural and thermodynamic properties that are dictated by the character of their intermolecular interactions.[1] Intermolecular forces include long-range electrostatic and dispersion interactions, as well as short-range Pauli repulsions and charge transfers, which have their origins in properties of the individual molecules (the electrical moments, polarizabilities, charge density, donor and acceptor levels, etc). Permanent electrostatics is by definition a pairwise additive effect, whilst induced electrostatics (polarization) depends on the local electric field on each molecule, which itself depends on how other nearby molecules are polarized, leading to many-body (i.e. cooperative or anticooperative) effects. Dispersion also includes significant many-body effects, whilst short-range Pauli repulsion and charge-transfer are predominantly two-body with small higher order corrections. Whilst the different long-range components of intermolecular interactions have textbook expressions in the non-overlapping regime,[1] computational tools such as energy decomposition analysis (EDA)[2] are needed to disentangle these contributions (and connect them to experimental observables) when there is overlap of molecular densities, as in complexes, clusters and the condensed phase.

In order to systematically explore the pairwise additive, and non-additive contributions to intermolecular interaction energies and forces, it is natural to examine the interaction energy of supramolecular systems using a many-body expansion (MBE), where the components are the individual molecules, i:

$$E_{tot} = \sum_{i}^{N} E_i + \sum_{i<j}^{N} \Delta E_{ij} + \sum_{i<j<k}^{N} \Delta E_{ijk} + \sum_{i<j<k<l}^{N} \Delta E_{ijkl} + \cdots \tag{1}$$

E_i are the energies of the single bodies, and ΔE_{ij}, ΔE_{ijk}, ΔE_{ijkl}, etc. are the two-body (2-B), three-body (3-B), and four-body (4-B), etc., interaction energies. The first two of

these are explicitly defined as:

$$\Delta E_{ij} = E_{ij} - E_i - E_j \tag{2}$$

$$\Delta E_{ijk} = E_{ijk} - E_{ij} - E_{ik} - E_{jk} + E_i + E_j + E_k \tag{3}$$

with similar construction for the higher order terms.

The utility of the MBE derives from the fact that even for strongly interacting molecules, intermolecular interactions are far weaker than intramolecular interactions (chemical bonds). Furthermore, since they decay either polynomially with distance (electrostatics and dispersion) or exponentially (Pauli repulsions and charge-transfer), the MBE exhibits reasonably rapid convergence.

The MBE has a long history which we cannot adequately do justice to here. Early on, 3-B contributions to dispersion were identified,[3,4] followed later by explorations of 3-B interactions in water.[5,6] Water exhibits large 3-B effects due to polarization (the effective dipole moment of water in the liquid is about 20% higher than in gas[7–9]). As computer power developed, the behavior of the MBE has been studied using computational quantum chemistry methods applied to diverse molecular clusters. Perhaps the most important of these are water clusters,[10–15] which established the significance of 3-B polarization effects. Water clusters containing ions such as halides,[16–18] alkali metal ions,[18,19] hydroxide,[20] and hydronium[21] have also been studied as models for many-body effects on ions in solution.

Cooperative, many-body effects (meaning $\geq$ 3-B) are naturally included in quantum mechanical (QM) calculations of interaction energies, but must be explicitly incorporated as part of molecular mechanics (MM) potentials.[22] Thus, one major motivation for understanding the many-body character of intermolecular interactions is to permit development of better MM potentials.[23,24] By contrast, early MM development focused on developing effective pair potentials[25] (for tractability). This was first performed for simple dispersion-

bound systems,[26,27] and then later for water and solutes in water where electrostatics are critical.[28] However, inclusion of non-additive terms is essential for describing heterogeneous environments (i.e., for transferability) and is driving the development of polarizable MM force fields which build in that most important cooperative effect.[24,29–31] The MBE is also the foundation of fragment-based quantum chemistry.[32,33]

From the view-point of understanding cooperative effects[34,35] in complex chemical environments, it is natural to ask how the 2-B interaction between a pair of tagged molecules, A and B, ΔE_{AB}, is modified by the presence of other molecules to become $\Delta E_{AB}^{\rm eff}$. The definition of cooperative effects, $\Delta E_{AB}^{\rm coop}$ on the $A-B$ interaction is simply:

$$\Delta E_{AB}^{\rm coop} = \Delta E_{AB}^{\rm eff} - \Delta E_{AB} \tag{4}$$

Comparing ΔE_{AB} against $\Delta E_{AB}^{\rm eff}$ addresses, for example, how the direct interaction of two ions is screened by a solvent, or how the interaction of a first solvent shell molecule with a solute is mediated by the presence of the remainder of the first solvation shell. Beyond the history, and the on-going MM developments touched on already, cooperative effects in non-bonded interactions are a subject of intense interest.[34] Some further reasons for this interest include understanding cooperative binding,[34,36,37] control over supramolecular chemistry and self-assembly,[38] and the ability to direct chemistry and catalysis through local electric fields[39,40] or other means.[41,42]

With characterizing cooperativity as the goal, this paper presents what we believe to be a new approach to evaluating the effective 2-B interaction, $\Delta E_{AB}^{\rm eff}$, between 2 tagged molecules in a complex system. $\Delta E_{AB}^{\rm eff}$ is defined such that the MBE terminates at the 2-B term. In other words:

$$E_{tot} = \sum_{i}^{N} E_i + \sum_{i<j}^{N} \Delta E_{ij}^{\rm eff} \tag{5}$$

In Section 2, a family of expressions are developed which systematically converge to $\Delta E_{AB}^{\rm eff}$,

such that correctness through P^{th} order of the MBE is obtained while performing only $\mathcal{O}(N^{P-3})$ separate calculations. In other words, to evaluate $\Delta E_{AB}^{\text{eff}}$ correct through 3rd order requires only $\mathcal{O}(N^0)$ calculations, whilst 4th order correctness requires only $\mathcal{O}(N^1)$ separate calculations, and so on. This approach is convenient, as well as efficient, if one is only interested in one or a few pairwise interactions.

With the theory in hand, its application to the environment effect on a model of the water-water hydrogen bond[43] is examined in Sub-section 3.1. This model adds 6 solvating H_2O molecules to a central dimer. It is interesting to revisit this model to address the practical issue of error analysis in the family of approximate expressions for $\Delta E_{AB}^{\text{eff}}$, not least because the previous study[43] used an expression which turns out to be only correct through second order in the MBE. The last part of the paper, Sub-section 3.2, considers the use of $\Delta E_{AB}^{\text{eff}}$ to analyze solvent effects on HCl dissociation in a small $(H_2O)_4$ cluster. This nanodroplet is interesting because it appears to be the smallest cluster in which HCl dissociation can occur.[44–46]

2 Methods

Our goal is to define the effective pairwise interaction energy, $\Delta E_{AB}^{\text{eff}}$, between two tagged molecules within the system in such a way that Eq. 5 is satisfied. Of course one will not want to *exactly* evaluate Eq. 5 as this would require explicit treatment of all interactions through N-body. Instead it is better to seek a family of expressions that are correct through a given order, P in the MBE. Such an expression will be denoted as $\Delta E_{AB}^{\text{eff}}(P)$. We shall present two families of valid expressions for $\Delta E_{AB}^{\text{eff}}(P)$; one that follows directly from the MBE, and one that looks superficially quite different.

Comparing Eqs. 1 and 5, it is evident that a definition of $\Delta E_{AB}^{\text{eff}}$ directly from the MBE

is:

$$\Delta E_{AB}^{\text{eff}} = \Delta E_{AB} + \frac{1}{3}\sum_{k_1 \neq A,B} \Delta E_{ABk_1} + \frac{1}{6}\sum_{k_1<k_2 \neq A,B} \Delta E_{ABk_1k_2} + \cdots$$
$$= \sum_{p=2}^{N} \frac{2}{p(p-1)} \sum_{k_1<k_2<\ldots<k_{(p-2)} \neq A,B} \Delta E_{ABk_1k_2\cdots k_{(p-2)}} \quad (6)$$

The prefactors for each p-body contribution ensure that Eq. 5 is satisfied. For example, one third of a given 3-B contribution is assigned equally to each of the 3 pairs within the "ABk_1" subsystems (three possible pairs); one sixth of the 4-B increments is assigned to each of the 6 pairs contained within the "ABk_1k_2" subsystems, etc. Truncation of Eq. 6 order by order gives rise to a sequence of approximate expressions, complete through P^{th} order ($P \geq 3$) in the MBE:

$$\Delta E_{AB}^{\text{eff}}(P) = \sum_{p=2}^{P} \frac{2}{p(p-1)} \sum_{k_1<k_2<\ldots<k_{(p-2)} \neq A,B} \Delta E_{ABk_1k_2\cdots k_{(p-2)}} \quad (7)$$

At lowest order, $P = 3$, there are $\mathcal{O}(N)$ 3-B contributions that correct each direct $A-B$ interaction, followed by $\mathcal{O}(N^2)$ 4-B interactions at $P = 4$, and so on. A and B are naturally chosen to be the two atoms or molecules of interest.

Likewise the environment is most logically treated as the other distinguishable molecules of the cluster or condensed phase environment, as implicitly assumed above. However, it is also possible to lump together everything that is not A and B into a single composite body that is their environment, R (the "rest" of the system). Indeed, it has been suggested[43] that the following easy-to-evaluate quantity:

$$\Delta E_{AB}^{\text{env}} \equiv E_{ABR} - E_{AR} - E_{BR} + E_R \quad (8)$$

will capture the effective two-body $A-B$ interaction. This is an appealing expression, which is trivially correct through second order, as shown by setting $R = 0$. However, no analysis

of its accuracy to higher orders has been presented.

To properly analyze Eq. 8 in terms of higher orders of the MBE, one can expand the environment, R into its component molecules, leading to:

$$\begin{aligned}\Delta E_{AB}^{\text{env}} = E_{AB} - E_A - E_B + \sum_k E_{ABk} - E_{Ak} - E_{Bk} + E_k \\ + \sum_{k<l} E_{ABkl} - E_{Akl} - E_{Bkl} + E_{kl} + \cdots\end{aligned} \tag{9}$$

Comparing equivalent p-body contributions to Eq. 9 against the corresponding contributions to the *exact* effective interaction energy, $\Delta E_{AB}^{\text{eff}}$, given in Eq. 6, it can be seen that the p-body terms in $\Delta E_{AB}^{\text{env}}$ are overcounted by factors of $\binom{p}{2}$. Specifically, while the second order term is correct, the 3-B contributions are overcounted by a factor of three. Thus, use of $\Delta E_{AB}^{\text{env}}$ is worse than not correcting the 3-B interactions at all (i.e., approximating the cooperative energy as zero is better than overestimating its leading terms by a factor of three). The situation at higher orders will be worse: for instance, the 4-B terms will be overcounted by a factor of 6. Direct use of Eq. 8 is clearly not a good idea.

However, a modified expression that is correct through 3$^{\text{rd}}$ order in the MBE, $\Delta E_{AB}^{\text{eff}}(3)'$, can be obtained easily. We take 1/3 of $\Delta E_{AB}^{\text{env}}$ to capture the 3-B terms correctly, which in turn captures 1/3 of the 2-B terms. We then explicitly add the remaining 2/3 of the 2-B terms to be complete through 3$^{\text{rd}}$ order:

$$\Delta E_{AB}^{\text{eff}}(3)' = \frac{1}{3}\Delta E_{AB}^{\text{env}} + \frac{2}{3}\Delta E_{AB} \tag{10}$$

Eq. 10 maintains the appealing aspect of Eq. 8, which is that regardless of system size, only a constant number of separate calculations are required. The new total is 7, consisting of 4 to evaluate Eq. 8, and an additional 3 for the 2-B interaction itself, ΔE_{AB}. By contrast, for an N-molecule system, $4N-5$ separate calculations are required to directly evaluate the

original 3rd order expression:

$$\Delta E_{AB}^{\text{eff}}(3) = \Delta E_{AB} + \frac{1}{3}\sum_{k\neq A,B} \Delta E_{ABk} \tag{11}$$

This process can be continued for the higher p-body terms. Eq. 10 has its leading error in the 4-B terms, which are overcounted by a factor of two (i.e. $6 \cdot \frac{1}{3}$). Thus we can take $1/2$ of $\Delta E_{AB}^{\text{eff}}(3)'$ to capture the 4-B terms fully, as well as half the lower order terms. Augmenting with $\frac{1}{2}\Delta E_{AB}^{\text{eff}}(3)$ provides the other half, leading to:

$$\Delta E_{AB}^{\text{eff}}(4)' = \frac{1}{2}\Delta E_{AB}^{\text{eff}}(3)' + \frac{1}{2}\Delta E_{AB}^{\text{eff}}(3) \tag{12}$$

Evidently evaluation of Eq. 12 requires $(4N-1)$ separate calculations as opposed to the $\mathcal{O}(N^2)$ separate calculations required to evaluate $\Delta E_{AB}^{\text{eff}}(4)$. It has its leading error in the 5-B terms.

With some additional algebra, it can be shown that the higher order corrections can be written recursively as

$$\Delta E_{AB}^{\text{eff}}(P)' = \frac{P-2}{P}\Delta E_{AB}^{\text{eff}}(P-1)' + \frac{2}{P}\Delta E_{AB}^{\text{eff}}(P-1) \tag{13}$$

The recursion is valid for $P \geq 3$, starting from the base case, namely $\Delta E_{AB}^{\text{eff}}(2)' \equiv \Delta E_{AB}^{\text{env}}$. P is of course the order in the MBE to which the expression is correct. Unrolling the recursion, we see that $\Delta E_{AB}^{\text{eff}}(P)'$ involves calculating E_{ABR}, E_{AR}, E_{BR}, and E_R first (i.e., the environment interactions), irrespective of the target order (P) of the effective 2-B energy. Then, for the desired P-body accuracy, all MBE terms $p \leq (P-1)$ containing *both* A and B need to be calculated. This contrasts with the direct evaluation of $\Delta E_{AB}^{\text{eff}}(P)$ via Eq. 6, which requires all MBE terms $p \leq P$ containing both A and B.

Likewise, a general expression for the leading error in the $(P+1)$-body terms associated

with $\Delta E_{AB}^{\rm eff}(P)'$ is given by:

$$\Delta E_{AB}^{\rm eff}(P)' - \Delta E_{AB}^{\rm eff}(P+1) = \frac{4}{(P-1)P(P+1)} \sum_{k_1<k_2<\ldots<k_{(P-1)} \neq A,B} \Delta E_{ABk_1k_2\cdots k_{(P-1)}} + \cdots \quad (14)$$

Alternatively, expressed as a ratio, the $(P+1)$-body terms are overcounted in $\Delta E_{AB}^{\rm eff}(P)'$ by a factor of:

$$F_P = \frac{(P+1)}{(P-1)} \quad (15)$$

This overcounting diminishes as $F_2 = 3$, $F_3 = 2$, $F_4 = \frac{5}{3}$, etc, as P is increased.

3 Results

3.1 Convergence of the effective 2-body interaction energy for a model water-water hydrogen bond

The effect of environment on the hydrogen bond between water molecules has been extensively analyzed via statistical mechanical theory and simulations. For example, the O-O radial distribution function, $g(r_{\text{O-O}})$, relates to the thermal average of an orientationally averaged effective pair potential, $v(r_{\text{O-O}})$.[47,48] Alternatively, the detailed anisotropic effect of a given environment on the hydrogen bond between a pair of tagged water molecules can be examined via the effective 2-B interaction energy theory presented above. Here we adopt a model $(H_2O)_8$ cluster used previously for this purpose,[43] which completes the first solvation shell of a central dimer with 3 additional H_2O molecules in a tetrahedral geometry per central H_2O. The resulting structure is provided in Figure 1 (see also Figures 2 and 4 of Ref. 43). Single point energy calculations are performed here using the def2-TZVPPD[49,50] basis set with the ωB97X-V density functional[51] (which is known to perform very well for non-covalent interactions[52,53]). All calculations were performed with the Q-Chem program

package.[54]

Figure 1 (bottom panel) presents the (exact) effective 2-B interaction energy (i.e. Eq. 6) of the reference hydrogen bond as a function of coordination shell size, n. With n ranging from the bare dimer ($n = 0$), to one environment molecule (six possible choices), two environment molecules (15 choices), etc, through six environment molecules. This same analysis was performed in Ref. 43, with the critical difference that cooperative effects were evaluated via Eq. 8, which is only correct through second order in the MBE, and overcounts the 3-B terms by a factor of three. Use of Eq. 8 is reproduced in the upper panel of Figure 1, and strong differences with the exact expression for $\Delta E_{AB}^{\text{eff}}$ are visually evident. Indeed the deviations (a mean absolute error of 4.1 kJ/mol and maximum error of 10.1 kJ/mol), and are larger than the errors that would arise from simply using the $n = 0$ value. These large errors associated with use of Eq. 8 to approximate $\Delta E_{AB}^{\text{eff}}$ are as anticipated, and indicate a substantial overestimation of the effects of the environment.

Nevertheless, the correct values of $\Delta E_{AB}^{\text{eff}}$ display the same trends as use of $\Delta E_{AB}^{\text{env}}$, and so *qualitative* conclusions from Ref. 43 remain valid. The addition of the first solvent molecule ($n = 1$) shows positive cooperativity (i.e. a strengthened H-bond) when an oxygen of the solvent molecule couples to the hydrogen of the acceptor water molecule (left water of the central dimer in Fig. 1), or a proton donor of the solvent molecule couples to the oxygen of the donor water (right water of the central dimer in Fig. 1). In order to explore the origin of the cooperativity effects, the effective 2-B interaction energy can also be broken down into separate physical components via a variational energy decomposition analysis (EDA) using absolutely localized orbitals.[2,55] EDA is applied here to separate $\Delta E_{AB}^{\text{eff}}$ values from the bottom panel of Fig. 2 into effective frozen (Pauli exclusion + electrostatics + dispersion), polarization, and charge transfer (CT) contributions. The positive cooperativity has its origin in enhanced polarization (through dipole alignment) and charge-transfer (through forming a water wire).

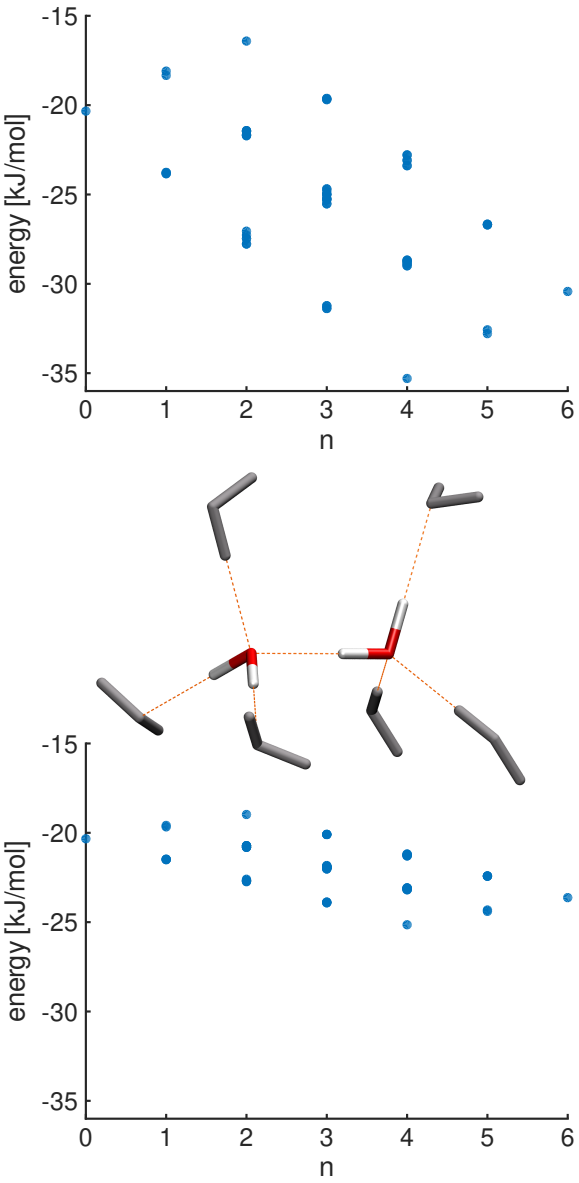

Figure 1: Effective 2-B interaction energy of the reference hydrogen bond in a model cluster as a function of the number of coordinating water molecules (the local environment), n, which range from 0 to 6.
Top: Use of Eq. 8, $\Delta E_{AB}^{\text{env}}$, to model the effective 2-B interaction energy, following reference 43.
Bottom: Exact evaluation of the effective 2-B interaction energy, $\Delta E_{AB}^{\text{eff}}$, via Eq. 6. Large differences relative to the approximation used in the top panel can be seen.
Inset: The geometry of the model $(H_2O)_8$ cluster from reference 43, which consists of a central H_2O dimer whose hydrogen bond interaction is modulated by up to 6 solvating water molecules (shown in grey) that complete the first solvent shell of the dimer.

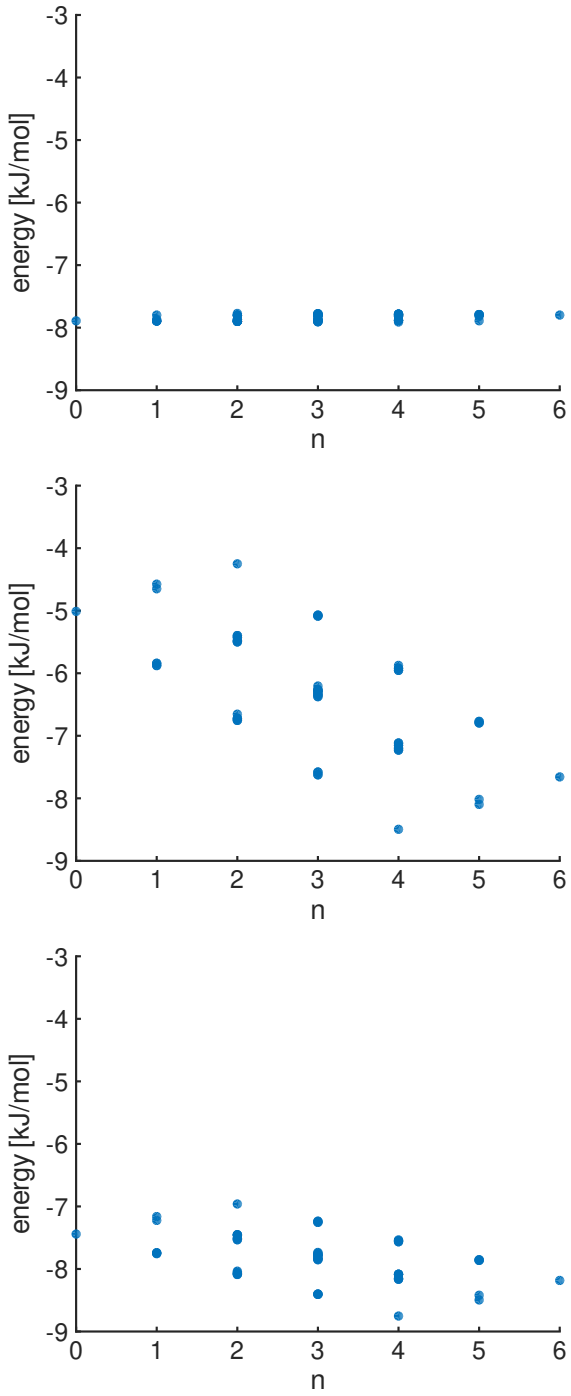

Figure 2: Energy decomposition analysis (EDA) of the effective two-body interactions from the bottom panel of Fig. 1. From top to bottom: frozen energy, polarization energy and charge transfer contributions. The sum of these contributions (which are all attractive) yields the total effective two-body interaction energy. It is evident that cooperativity and anticooperativity effects are strongest for the polarization contribution, and those for charge transfer track those for polarization.

There is negative cooperativity (i.e. a weakened H-bond) when a hydrogen of the solvent molecule couples to the oxygen of the acceptor water molecule, or the oxygen of a solvent molecule couples to a hydrogen of the donor water. Negative cooperativity has its origin in attenuated polarization (through dipole anti-alignment) and diminished charge-transfer (through forward CT to a single water molecule from two others). While CT is a larger contributor to the effective 2-B interaction energy than polarization, it is only moderately sensitive to cooperativity. Polarization however, is found to be the most sensitive to cooperativity. Starting at $n = 4$, polarization begins to compete with CT for dominance, and by $n = 6$ they are nearly equal. Conversely, the frozen contribution is found to have comparatively little to no cooperativity. The balance of contributions mirrors those reported previously:[14,56] no single term dominates the hydrogen bond, although the largest many-body effects are due to polarization.

Let us turn next to an assessment of the errors incurred by approximating $\Delta E_{AB}^{\text{eff}}$ by the approximate expressions, $\Delta E_{AB}^{\text{eff}}(3)'$ (Eq. 10), $\Delta E_{AB}^{\text{eff}}(4)'$ (Eq. 12), and the general result, $\Delta E_{AB}^{\text{eff}}(P)'$ (Eq. 13). In order to estimate an acceptable choice of order, P, for the effective 2-B energy calculation, the mean absolute error over coordination numbers from $n = 1 - 6$ is evaluated here for each order, $P = 2 - 7$ (of course when $P = n$ it is exact). Figure 3 plots the MAE in kJ/mol for each order ($\Delta E_{AB}^{\text{eff}}(P)'$ and $\Delta E_{AB}^{\text{eff}}(P)$) as a function of cluster size relative to $\Delta E_{AB}^{\text{eff}}(8)$ (note $\Delta E_{AB}^{\text{eff}}(8)$ equals $\Delta E_{AB}^{\text{eff}}(8)'$ in this example, i.e., at the full system size). A drop of two orders of magnitude in the MAE is observed when moving from $\Delta E_{AB}^{\text{eff}}(2)'$ to $\Delta E_{AB}^{\text{eff}}(3)'$ (4.1 kJ/mol to 0.047 kJ/mol), followed by drops of roughly one order of magnitude for every increase in P beyond three. A slight increase in error is observed for increasing cluster size. This is to be expected, since the error originates from overcounting the higher order contributions, and larger systems have many more higher body terms. From this analysis, $P = 3$ can be seen to be already useful, and $P = 4$ or certainly $P = 5$ should be adequate for computations. A similar pattern is observed for $\Delta E_{AB}^{\text{eff}}(P)$,

with order of magnitude drops in MAE between successive orders. Note that as anticipated, $\Delta E^{\text{eff}}_{AB}(2)$ performs quantitatively better than $\Delta E^{\text{eff}}_{AB}(2)'$, despite $\Delta E^{\text{eff}}_{AB}(2)$ containing zero environmental effects. At third order and beyond, both $\Delta E^{\text{eff}}_{AB}(P)'$ and $\Delta E^{\text{eff}}_{AB}(P)$ appear to perform similarly.

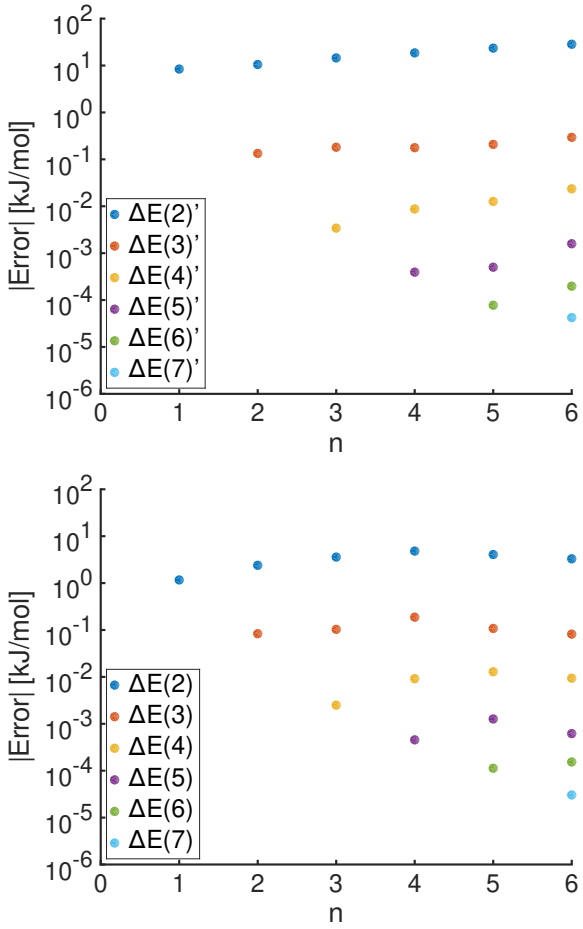

Figure 3: The errors associated with various orders of approximation, P, to the effective 2-B energies, $\Delta E^{\text{eff}}_{AB}$, for a central hydrogen bond in the model $(H_2O)_8$ cluster shown in Fig. 1, for each possible selection of a solvation shell of size $1 \leq n \leq 6$.
Top: $\Delta E^{\text{eff}}_{AB}(P)'$ (equation 13)
Bottom: $\Delta E^{\text{eff}}_{AB}(P)$ (equation 6)

3.2 Example application: Hydrated HCl clusters

As another example of using the effective 2-B interaction energies, we turn next to considering the role of solvation on a proton transfer pathway for dissociation of HCl in a cluster of stoichiometry $HCl(H_2O)_4$. Acid dissociation in H_2O is a fundamental process in chemistry, and a nanodroplet of HCl and four H_2O molecules is particularly interesting because it is believed to be the smallest system where structures with dissociated HCl are stable.[44–46,57–59] Even in a system as small as this, there are numerous local minima, and so we restrict our attention to a single well-defined reaction coordinate for proton transfer from HCl to H_2O. As illustrated in Figure 4 below, this is a relaxed potential energy scan where the distance $R(O\cdots H)$ (between the acidic proton and hydronium oxygen) is constrained to have values between 0.9 Å and 2.7 Å. The scan was performed at the ωB97M-V/def2-TZVPD level of theory, using the Q-Chem program package.[54] The cluster at $R(O\cdots H)$= 1.44 Å corresponds to the equilibrium structure of our selected isomer of undissociated $HCl(H_2O)_4$, where the proton-accepting water (W1) acts as a double H-bond donor and two water molecules (W3 and W4) form hydrogen-bonds with the chlorine atom (see annotated cluster in Figure 4). The fourth water molecule (W2) is not directly interacting with HCl, but completes the ring-like structure of the water tetramer.

For purposes of many-body expansion analysis, the cluster is regarded as being composed of six species: an H^+ cation, a Cl^- anion, and four neutral H_2O molecules. This choice of fragments acts as a necessary compromise, since a reference involving an HCl or hydronium ion fragment can only be well-defined for portions of the proton-transfer potential energy surface (PES). Since this system is undergoing a chemical reaction (i.e., acid dissociation), there is an important role for the interactions beyond 2-B, which can stabilize the separation of the ions. The total 2-B contribution is significantly greater than 100% of the total interaction energy (see Fig. 5). It is stronger (i.e., more negative) in the isolated pairs, with a maximum of 147%, and a value of 142% at equilibrium (vertical dashed line). The 3-B

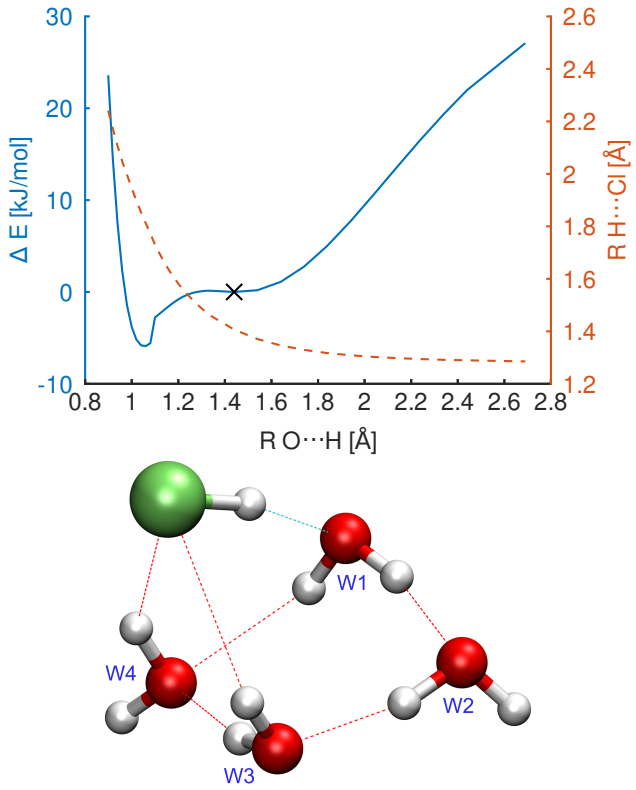

Figure 4: Top: Relaxed potential energy surface scan (blue) regarding the proton-transfer from HCl to W1 at the ωB97M-V/def2-TZVPD level of theory. The corresponding energies are given relative to the equilibrium structure of the undissociated cluster. Additionally, the H-Cl distance (orange) is shown for each point of the PES scan. Bottom: Equilibrium structure of the undissociated $HCl(H_2O)_4$ used in the main text. The blue labels refer to the individual water molecules.

contribution counteracts this bare 2-B term with a repulsive anti-binding contribution, that has a maximum value of -66%, and a value of -54% at equilibrium. The total 4-B contribution has a maximum value of 29%, and a value of 18% at equilibrium. The 5-B and 6-B total $\sim$ 5% together, and show only marginal dependence on the O$\cdots$H distance.

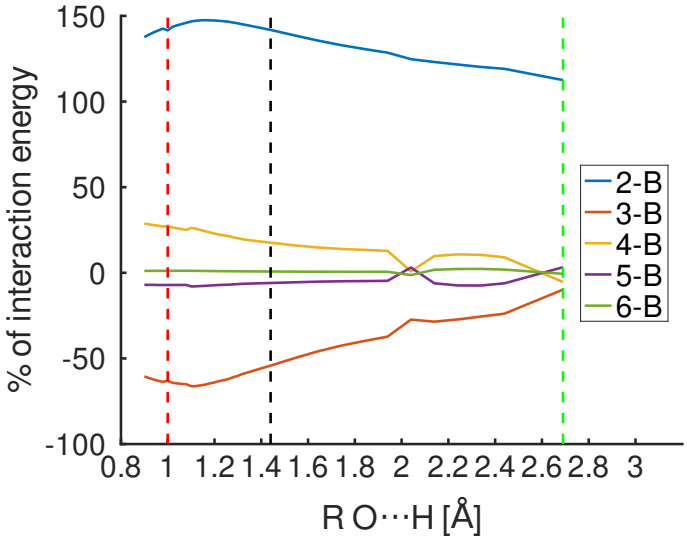

Figure 5: The percent contribution of the many-body terms to the total interaction energy of $HCl(H_2O)_4$ of a PES scan of a proton transfer. The red dashed line represents the strongest interacting hydronium cluster, the black dashed line is a stable undissociated equilibrium, and the green dashed line contains the shortest HCl bond observed.

The interaction energy change along this relaxed scan is relatively small, and is shown in the purple curve of Figure 6, indicating that the arrangement of the three solvating water molecules plays a critical role in stabilizing the otherwise quite unfavorable ion pair configuration. In order to illustrate this, a step-wise solvation is performed by incrementally incorporating each water molecule in its position at the cluster geometry, which does not involve a re-optimization of the PES. For clarity, only one possible step-wise solvation is shown: W2, W3, followed by W4. All other possible solvation sequences have similar trends, and the results can be found in the Supporting Information. The cluster geometries of the relaxed scan can also be found in the Supporting Information. Compared to the interaction of H^+ and Cl^-, the introduction of the proton-accepting water W1 lowers the interaction

energy overall, whereby the largest gain in interaction energy occurs in the dissociated regime (red dashed line) due to the stabilization of the bare proton by W1. The incorporation of W2 and W3 further lowers the total interaction energy and follows the same trend of stronger interactions in the dissociated regime as compared to the undissociated structures. Upon addition of W4 the interaction energy is for the first time lower for the dissociated cluster than the undissociated equilibrium structure. This finding supports the reported minimum number of four water molecules required for dissociation.[44–46]

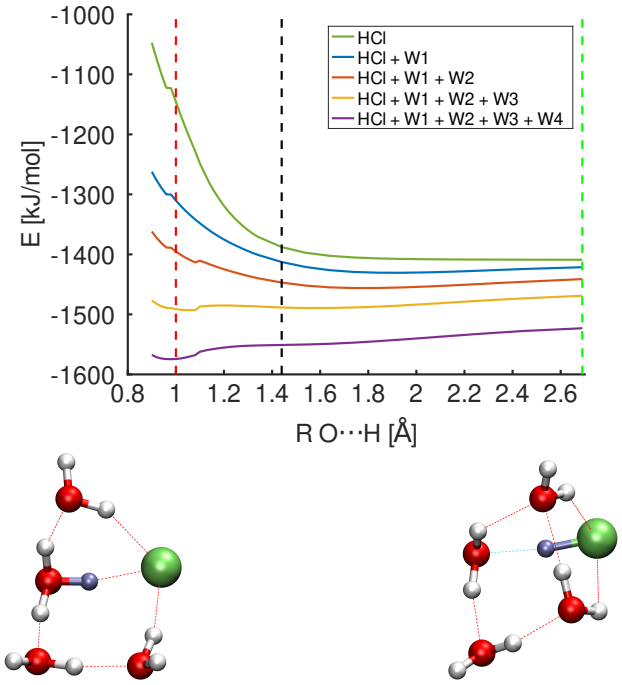

Figure 6: The total interaction energy of a PES scan of a proton transfer in an $HCl(H_2O)_4$ cluster. The individual curves represent successive solvations in the geometry of the cluster (see Figure 4, and text for details). The red dashed line represents the strongest interacting hydronium cluster, the black dashed line is a stable undissociated equilibrium, and the green dashed line contains the shortest HCl bond observed.

The role which the 3-B and 4-B, etc., contributions play in facilitating the proton transfer can be illustrated best through comparing effective 2-B interaction energies. Figure 7a plots the sum of the effective 2-B energies of the proton-transfer subsystem ($\Delta E^{\text{eff}}_{\text{Cl}^-\,\text{H}^+} + \Delta E^{\text{eff}}_{\text{Cl}^-\,\text{W1}} + \Delta E^{\text{eff}}_{\text{H}^+\,\text{W1}}$) as the solvation shell is filled.

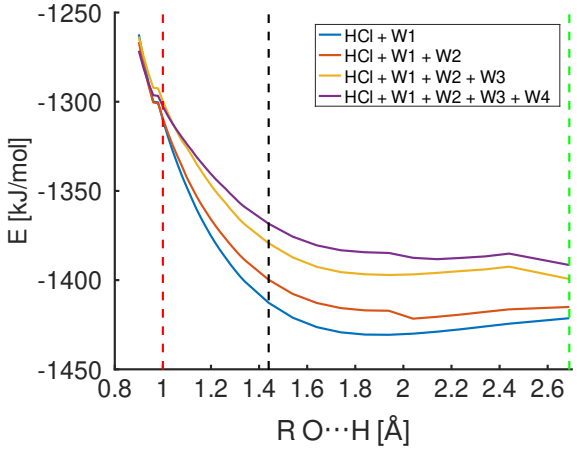

(a) Total effective 2-B energy of the solute subsystem $(Cl^- \cdots H^+ \cdots H_2O)$

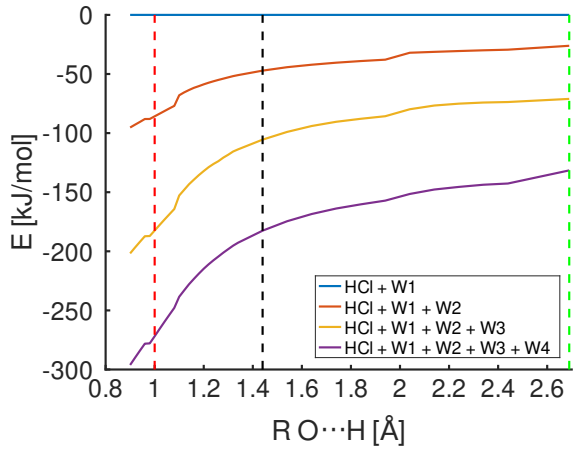

(b) Total effective 2-B energy of the solvent $((H_2O)_{n-1})$

Figure 7: The total effective 2-B energies of the PES of an $HCl(H_2O)_4$ cluster plotted for the solute (a) and solvent (b) separately. The individual curves represent successive solvation in the geometry of the full cluster (see Figure 4, and text for details). The red dashed line represents the strongest interacting hydronium cluster, the black dashed line is a stable undissociated equilibrium, and the green dashed line contains the shortest HCl bond observed. N.B., the sum of the curves of (a) and (b) equals the total interaction energies plotted in Figure 6.

As can be seen, the addition of solvating H_2O molecules does not stabilize the dissociated product within the sub-cluster of $Cl^- \cdots H^+ \cdots H_2O$. In fact, the solvation has the opposite effect, leading to an increase in the interaction energy with successive solvation; contrary to the total interaction energy observed in Figure 6.

Another interesting feature of Fig. 7a is that the effective interaction energy for the dissociated cluster ($r(\mathrm{OH}) = 1.0\,\text{Å}$) is almost independent of the number of spectator water molecules in the system. Closer inspection of the contributing terms finds that while the additional 3-B and higher order terms are non-zero, they cancel each other out in the dissociated regime. At the undissociated equilibrium structure ($r(\mathrm{OH}) = 1.44\,\text{Å}$) and larger O-H separations, however, the additional terms appearing in the effective 2-B energy do not cancel and are net positive leading to an attenuated effective interaction.

Although the effective interaction energy, i.e., sum of effective 2-B energies, in the proton-transfer subsystem becomes less stable with the addition of spectator water molecules, the difference with respect to the dissociated (red dashed line in Fig. 7) and undissociated (black dashed line) cluster geometry decreases. For the bare $Cl^- \cdots H^+ \cdots H_2O$ subsystem this difference amounts to 102.6 kJ/mol. Including interactions with spectator water W2, the difference reduces to 90.4 kJ/mol. Successively adding the two remaining water molecules (W3, W4) the difference is further reduced to 81.7 kJ/mol and 65.8 kJ/mol, respectively.

Figure 7b plots the sum of the effective 2-B energies of the solvating H_2O molecules along the PES with successive solvation. The effective interaction energies of the solvating H_2O molecules is found to decrease across all $O \cdots H$ distances, and across all degrees of solvation; although the decrease is greater at shorter $O \cdots H$ distances, and with higher solvation number. The difference in effective 2-B energy with respect to the dissociated (red dashed line in Fig. 7b) and undissociated (black dashed line) geometries with the addition of successive water molecules W2, W3, and W4, are -38.7, -74.3, and -89.3 kJ/mol respectively.

Conveniently, due to the definition of the effective 2-B interaction energies, the sum of the

individual curves of Figures 7a and 7b equals the individual curves of Figure 6. Therefore, the effective 2-B interaction energies effortlessly shows that the proton transfer is not being driven by the lowering of the energy of the proton transfer itself (Fig. 7a), but instead due to the lowering of the energy of the hydrogen-bond network (7b) in the presence of hydronium. Interestingly, at the dissociated limit, there is actually one less hydrogen-bond present, yet the interaction energy continues to increase, highlighting the importance of cooperativity in the hydrogen-bonds.

In other words, the dissociation of HCl is found to be increasingly unfavorable to the *solute*, but increasingly favorable to the *solvent* with increasing solvation. This mechanism suggests why the smallest nanodroplet size for HCl dissociation contains four H_2O molecules; the hydrogen bond network must be large enough such that the advantage to the network overcomes the disadvantage of HCl dissociation itself.

4 Conclusions

The main purpose of this paper was to use the many-body expansion (MBE) to define effective two-body (2-B) interaction energies in a molecular cluster or condensed phase system composed of molecules that interact via potentials that are not pairwise additive, such as the energies from quantum chemistry calculations or advanced force fields. The effective 2-B interaction energies, $\Delta E_{AB}^{\text{eff}}$, sum correctly to the total interaction energy at a given geometry, reflecting Eq. 5. We believe that examination of $\Delta E_{AB}^{\text{eff}}$ may be useful for various applications, such as understanding cooperativity effects on bare 2-B interactions, and how they vary from environment to environment. Additionally, the effective 2-B interaction energies allow for a straight forward, intuitive, description of higher n-body interactions; avoiding the arduous task of interpreting the myriad of higher order contributions.

Two classes of expressions were developed for $\Delta E_{AB}^{\text{eff}}$ which each achieve correctness to a

given target order, P in the MBE. One class, $\Delta E_{AB}^{\rm eff}(P)$, corresponds simply to truncating the MBE at P-th order and democratically dispersing the higher-body contributions to each pairwise contribution they are associated with. To find a particular effective 2-B interaction, $\Delta E_{AB}^{\rm eff}$, in a system of N molecules, the expression correct through 3rd order, $\Delta E_{AB}^{\rm eff}(3)$, involves $\mathcal{O}(N)$ separate calculations, while the expression correct through 4th order, $\Delta E_{AB}^{\rm eff}(4)$, requires $\mathcal{O}(N^2)$ separate calculations, and so on.

The other class of expressions for $\Delta E_{AB}^{\rm eff}(P)'$ is rather different and is based on a calculation on the whole system plus corrections on subsystems. Interestingly, the alternative expression correct through 3rd order, $\Delta E_{AB}^{\rm eff}(3)'$, involves only $\mathcal{O}(N^0)$ separate calculations, while the alternative expression correct through 4th order, $\Delta E_{AB}^{\rm eff}(4)'$, requires only $\mathcal{O}(N)$ separate calculations, and so on. Expressions for the leading error associated with truncation at P-th order are given.

A model $(H_2O)_8$ cluster that completes the first solvation shell around a central water-water hydrogen bond was used as a first example, and as a vehicle for evaluating the errors associated with truncating the two classes of expressions for $\Delta E_{AB}^{\rm eff}$ at finite order in the MBE: $P = 2, 3, 4 \ldots$. $P = 3$ is the first useful approximation, and $\Delta E_{AB}^{\rm eff}(3)'$ yields a mean absolute error (MAE) of 0.05 kJ/mol for the water clusters examined. $\Delta E_{AB}^{\rm eff}(4)'$ reduces those errors in the effective 2-B interaction energies by another factor of roughly 5-10, which yields errors below 0.01 kJ/mol for our test system.

An example application of the effective 2-B interaction energy is shown to be useful in describing the physics of a proton transfer in HCl + $(H_2O)_4$ cluster. The successive solvation of HCl + H_2O was found to remain disadvantageous for proton transfer, rather the energetic advantage was found to occur within the strengthening of the hydrogen-bond network itself. This points towards a possible mechanism to explain the minimum solvation shell size in order to dissociate HCl; the hydrogen-bond network must be large enough to become energetically advantageous over the disadvantageous HCl dissociation. Further investigation with various

cluster sizes and conformers using effective 2-B interaction energies is warranted in order to confirm this finding.

5 Supporting Information

Geometry of model water cluster. Plots of all solvation sequences of $HCl(H_2O)_4$ PES scans. Cluster geometries of $HCl(H_2O)_4$ PES scans.

6 Acknowledgements

This work was supported by funding from the National Institutes of Health under Grant No. 5U01GM121667, with additional support from the National Science Foundation, under Grant No. CHE-1955643. A.Z. gratefully acknowledges financial support from the Swiss National Science Foundation through the Early Postdoc.Mobility fellowship.

References

(1) Stone, A. J. *The Theory of Intermolecular Forces*, second edition ed.; Oxford University Press: Oxford, 2013.

(2) Mao, Y.; Loipersberger, M.; Horn, P. R.; Das, A.; Demerdash, O.; Levine, D. S.; Veccham, S. P.; Head-Gordon, T.; Head-Gordon, M. From intermolecular interaction energies and observable shifts to component contributions and back again: A tale of variational energy decomposition analysis. *Annu. Rev. Phys. Chem.* **2021**, *72*, 641–666.

(3) Axilrod, B. M.; Teller, E. Interaction of the van der Waals type between three atoms. *J. Chem. Phys.* **1943**, *11*, 299–300.

(4) Muto, Y. Force between nonpolar molecules. *J. Phys. Math. Soc. Japan* **1943**, *17*, 629.

(5) Hankins, D.; Moskowitz, J. W.; Stillinger, F. H. Hydrogen-bond energy nonadditivity in water. *Chem. Phys. Lett.* **1970**, *4*, 527–530.

(6) Hankins, D.; Moskowitz, J. W.; Stillinger, F. H. Water Molecule Interactions. *J. Chem. Phys.* **1970**, *53*, 4544–+.

(7) Hasted, J. B. In *The Physics and Physical Chemistry of Water*; Franks, F., Ed.; Springer New York: Boston, MA, 1972; pp 255–309.

(8) Silvestrelli, P. L.; Parrinello, M. Water Molecule Dipole in the Gas and in the Liquid Phase. *Phys. Rev. Lett.* **1999**, *82*, 3308–3311.

(9) Gubskaya, A. V.; Kusalik, P. G. The total molecular dipole moment for liquid water. *J. Chem. Phys.* **2002**, *117*, 5290–5302.

(10) Xantheas, S. S. Ab-Initio Studies of Cyclic Water Clusters (H2O)(N), N=1-6 .2. Analysis of Many-Body Interactions. *J. Chem. Phys.* **1994**, *100*, 7523–7534.

(11) Xantheas, S. S. Cooperativity and hydrogen bonding network in water clusters. *Chem. Phys.* **2000**, *258*, 225–231.

(12) Cui, J.; Liu, H. B.; Jordan, K. D. Theoretical characterization of the (H2O)(21) cluster: Application of an n-body decomposition procedure. *J. Phys. Chem. B* **2006**, *110*, 18872–18878.

(13) Góra, U.; Podeszwa, R.; Cencek, W.; Szalewicz, K. Interaction energies of large clusters from many-body expansion. *J. Chem. Phys.* **2011**, *135*, 224102.

(14) Cobar, E. A.; Horn, P. R.; Bergman, R. G.; Head-Gordon, M. Examination of the hydrogen-bonding networks in small water clusters (n=2-5, 13, 17) using absolutely localized molecular orbital energy decomposition analysis. *Phys. Chem. Chem. Phys.* **2012**, *14*, 15328–15339.

(15) Heindel, J. P.; Xantheas, S. S. The Many-Body Expansion for Aqueous Systems Revisited: I. Water-Water Interactions. *J. Chem. Theory Comput.* **2020**, *16*, 6843–6855.

(16) Xantheas, S. S. Quantitative description of hydrogen bonding in chloride-water clusters. *J. Phys. Chem.* **1996**, *100*, 9703–9713.

(17) Bizzarro, B. B.; Egan, C. K.; Paesani, F. Nature of Halide-Water Interactions: Insights from Many-Body Representations and Density Functional Theory. *J. Chem. Theory Comput.* **2019**, *15*, 2983–2995.

(18) Heindel, J. P.; Xantheas, S. S. The Many-Body Expansion for Aqueous Systems Revisited: II. Alkali Metal and Halide Ion-Water Interactions. *J. Chem. Theory Comput.* **2021**, *17*, 2200–2216.

(19) Egan, C. K.; Bizzarro, B. B.; Riera, M.; Paesani, F. Nature of Alkali Ion-Water Interactions: Insights from Many-Body Representations and Density Functional Theory. II. *J. Chem. Theory Comput.* **2020**, *16*, 3055–3072.

(20) Egan, C. K.; Paesani, F. Assessing Many-Body Effects of Water Self-Ions. I: OH-(H2O) n Clusters. *J. Chem. Theory Comput.* **2018**, *14*, 1982–1997.

(21) Egan, C. K.; Paesani, F. Assessing Many-Body Effects of Water Self-Ions. II: H3O+(H2O) n Clusters. *J. Chem. Theory Comput.* **2019**, *15*, 4816–4833.

(22) Albaugh, A.; Boateng, H. A.; Bradshaw, R. T.; Demerdash, O. N.; Dziedzic, J.; Mao, Y. Z.; Margul, D. T.; Swails, J.; Zeng, Q.; Case, D. A.; et al, Advanced Potential Energy Surfaces for Molecular Simulation. *J. Phys. Chem. B* **2016**, *120*, 9811–9832.

(23) Demerdash, O.; Mao, Y. Z.; Liu, T. Y.; Head-Gordon, M.; Head-Gordon, T. Assessing many-body contributions to intermolecular interactions of the AMOEBA force field

using energy decomposition analysis of electronic structure calculations. *J. Chem. Phys.* **2017**, *147*, 161721.

(24) Lambros, E.; Paesani, F. How good are polarizable and flexible models for water: Insights from a many-body perspective. *J. Chem. Phys.* **2020**, *153*, 060901.

(25) Stillinger, F. H. Density Expansions For Effective Pair Potentials. *J. Chem. Phys.* **1972**, *57*, 1780–+.

(26) Kestner, N. R.; Sinanoglu, O. Effective Intermolecular Pair Potentials In Nonpolar Media. *J. Chem. Phys.* **1963**, *38*, 1730–1739.

(27) Sinanoglu, O. An intermolecular potential for use in liquids. *Chem. Phys. Lett.* **1967**, *1*, 340–342.

(28) Stillinger, F. H. Effective Pair Interactions In Liquids - Water. *J. Phys. Chem.* **1970**, *74*, 3677–+.

(29) Ren, P. Y.; Ponder, J. W. Polarizable atomic multipole water model for molecular mechanics simulation. *J. Phys. Chem. B* **2003**, *107*, 5933–5947.

(30) Ponder, J. W.; Wu, C. J.; Ren, P. Y.; Pande, V. S.; Chodera, J. D.; Schnieders, M. J.; Haque, I.; Mobley, D. L.; Lambrecht, D. S.; DiStasio, R. A.; et al, Current Status of the AMOEBA Polarizable Force Field. *J. Phys. Chem. B* **2010**, *114*, 2549–2564.

(31) Das, A. K.; Urban, L.; Leven, I.; Loipersberger, M.; Aldossary, A.; Head-Gordon, M.; Head-Gordon, T. Development of an Advanced Force Field for Water Using Variational Energy Decomposition Analysis. *J. Chem. Theory Comput.* **2019**, *15*, 5001–5013.

(32) Gordon, M. S.; Fedorov, D. G.; Pruitt, S. R.; Slipchenko, L. V. Fragmentation Methods: A Route to Accurate Calculations on Large Systems. *Chem. Rev.* **2012**, *112*, 632–672.

(33) Herbert, J. M. Fantasy versus reality in fragment-based quantum chemistry. *J. Chem. Phys.* **2019**, *151*, 170901.

(34) Mahadevi, A. S.; Sastry, G. N. Cooperativity in Noncovalent Interactions. *Chem. Rev.* **2016**, *116*, 2775–2825.

(35) Tebben, L.; Muck-Lichtenfeld, C.; Fernandez, G.; Grimme, S.; Studer, A. From Additivity to Cooperativity in Chemistry: Can Cooperativity Be Measured? *Chem. Eur. J* **2017**, *23*, 5864–5873.

(36) Robertson, A.; Shinkai, S. Cooperative binding in selective sensors, catalysts and actuators. *Coord. Chem. Rev.* **2000**, *205*, 157–199.

(37) Saha, S.; Sastry, G. N. Cooperative or Anticooperative: How Noncovalent Interactions Influence Each Other. *J. Phys. Chem. B* **2015**, *119*, 11121–11135.

(38) Ercolani, G. Assessment of cooperativity in self-assembly. *J. Am. Chem. Soc.* **2003**, *125*, 16097–16103.

(39) Mafé, S.; Ramírez, P.; Alcaraz, A. Electric field-assisted proton transfer and water dissociation at the junction of a fixed-charge bipolar membrane. *Chem. Phys. Lett.* **1998**, *294*, 406–412.

(40) Rokob, T. A.; Bakó, I.; Stirling, A.; Hamza, A.; Pápai, I. Reactivity models of hydrogen activation by frustrated Lewis pairs: synergistic electron transfers or polarization by electric field? *J. Am. Chem. Soc.* **2013**, *135*, 4425–4437.

(41) Haak, R. M.; Wezenberg, S. J.; Kleij, A. W. Cooperative multimetallic catalysis using metallosalens. *Chem. Commun.* **2010**, *46*, 2713–2723.

(42) Lather, J.; Bhatt, P.; Thomas, A.; Ebbesen, T. W.; George, J. Cavity Catalysis by Cooperative Vibrational Strong Coupling of Reactant and Solvent Molecules. *Angew. Chem. Int. Ed. Engl.* **2019**, *58*, 10635–10638.

(43) Hus, M.; Urbic, T. Strength of hydrogen bonds of water depends on local environment. *J. Chem. Phys.* **2012**, *136*, 144305.

(44) Gutberlet, A.; Schwaab, G.; Birer, O.; Masia, M.; Kaczmarek, A.; Forbert, H.; Havenith, M.; Marx, D. Aggregation-Induced Dissociation of HCl(H2O)4 Below 1 K: The Smallest Droplet of Acid. *Science* **2009**, *324*, 1545–1548.

(45) Vargas-Caamal, A.; Cabellos, J. L.; Ortiz-Chi, F.; Rzepa, H. S.; Restrepo, A.; Merino, G. How Many Water Molecules Does it Take to Dissociate HCl? *Chem. Eur. J* **2016**, *22*, 2812–2818.

(46) Mani, D.; de Tudela, R. P.; Schwan, R.; Pal, N.; Körning, S.; Forbert, H.; Redlich, B.; van der Meer, A. F. G.; Schwaab, G.; Marx, D.; et al, Acid solvation versus dissociation at "stardust conditions": Reaction sequence matters. *Sci. Adv.* **2019**, *5*, eaav8179–eaav8179.

(47) Henderson, R. L. Uniqueness theorem for fluid pair correlation-functions. *Phys. Lett. A* **1974**, *49*, 197–198.

(48) Johnson, M. E.; Head-Gordon, T.; Louis, A. A. Representability problems for coarse-grained water potentials. *J. Chem. Phys.* **2007**, *126*, 144509.

(49) Weigend, F.; Ahlrichs, R. Balanced basis sets of split valence, triple zeta valence and quadruple zeta valence quality for H to Rn: Design and assessment of accuracy. *Phys. Chem. Chem. Phys.* **2005**, *7*, 3297–3305.

(50) Rappoport, D.; Furche, F. Property-optimized Gaussian basis sets for molecular response calculations. *J. Chem. Phys.* **2010**, *133*, 134105.

(51) Mardirossian, N.; Head-Gordon, M. ωB97X-V: A 10-parameter, range-separated hybrid, generalized gradient approximation density functional with nonlocal correlation, designed by a survival-of-the-fittest strategy. *Phys. Chem. Chem. Phys.* **2014**, *16*, 9904–9924.

(52) Mardirossian, N.; Head-Gordon, M. Thirty years of density functional theory in computational chemistry: an overview and extensive assessment of 200 density functionals. *Mol. Phys.* **2017**, *115*, 2315–2372.

(53) Goerigk, L.; Hansen, A.; Bauer, C.; Ehrlich, S.; Najibi, A.; Grimme, S. A look at the density functional theory zoo with the advanced GMTKN55 database for general main group thermochemistry, kinetics and noncovalent interactions. *Phys. Chem. Chem. Phys.* **2017**, *19*, 32184–32215.

(54) Shao, Y.; Gan, Z.; Epifanovsky, E.; Gilbert, A. T. B.; Wormit, M.; Kussmann, J.; Lange, A. W.; Behn, A.; Deng, J.; Feng, X.; et al, Advances in molecular quantum chemistry contained in the Q-Chem 4 program package. *Mol. Phys.* **2015**, *113*, 184–215.

(55) Horn, P. R.; Mao, Y.; Head-Gordon, M. Probing non-covalent interactions with a second generation energy decomposition analysis using absolutely localized molecular orbitals. *Phys. Chem. Chem. Phys.* **2016**, *18*, 23067–23079.

(56) Khaliullin, R. Z.; Bell, A. T.; Head-Gordon, M. Electron Donation in the Water-Water Hydrogen Bond. *Chem. Eur. J* **2009**, *15*, 851–855.

(57) Boda, M.; Naresh Patwari, G. Insights into acid dissociation of HCl and HBr with internal electric fields. *Phys. Chem. Chem. Phys.* **2017**, *19*, 7461–7464.

(58) Bresnahan, C. G.; David, R.; Milet, A.; Kumar, R. Ion Pairing in HCl–Water Clusters: From Electronic Structure Investigations to Multiconfigurational Force-Field Development. *J. Phys. Chem. A* **2019**, *123*, 9371–9381, PMID: 31589444.

(59) Christensen, E. G.; Steele, R. P. Stepwise Activation of Water by Open-Shell Interactions, Cl(H2O)n=4–8,17. *J. Phys. Chem. A* **2020**, *124*, 3417–3437, PMID: 32243169.

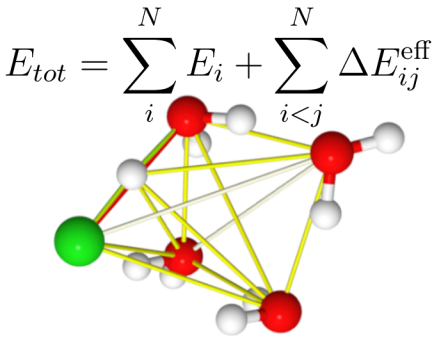

Figure 8: TOC Graphic